https://doi.org/10.5194/tc-2022-191
Preprint. Discussion started: 4 October 2022

The Cryosphere Discussions

Evaluation of snow depth retrievals from ICESat-2 using airborne laser-scanning data

César Deschamps-Berger[1,2], Simon Gascoin[1], David Shean[3], Hannah Besso[3], Ambroise Guiot[1], Juan Ignacio López-Moreno[2]

[1]Centre d'Etudes Spatiales de la Biosphère, CESBIO, Univ. Toulouse, CNES/CNRS/INRAE/IRD/UPS, Toulouse, France.
[2]Instituto Pirenaico de Ecología, Consejo Superior de Investigaciones Científicas (IPE-CSIC), Zaragoza, Spain
[3]University of Washington, Dept. of Civil and Environmental Engineering, Seattle, WA

Correspondence to: César Deschamps-Berger (cesar.deschamps-berger@csic.es)

Abstract. The unprecedented precision of the altimetry satellite ICESat-2 and the increasing availability of high-resolution elevation datasets open new opportunities to measure snow depth in mountains, a critical variable for ecosystems and water resources monitoring. We retrieved snow depth over the upper Tuolumne basin (California, USA) for three years by differencing ICESat-2 ATL06 snow-on elevations and various snow-off elevation sources, including ATL06 and external digital elevation models. Snow depth derived from ATL06 data only (snow-on and snow-off) provided a poor temporal and spatial coverage, limiting its utility. However, using airborne lidar or satellite photogrammetry elevation models as snow-off elevation source yielded an accuracy of ~0.2 m (bias), a precision of ~0.5 m for low slopes and ~1.2 m for steeper areas, compared to eight reference airborne lidar snow depth maps. The snow depth derived from ICESat-2 ATL06 will help address the challenge of measuring the snow depth in unmonitored mountainous areas.

1 Introduction

Seasonal snow cover provides fresh water resources to over a billion people globally (Barnett et al., 2005; Sturm et al., 2017). The spatial distribution of the mass of snow on the ground (snow water equivalent, SWE) in snow dominated catchments is key information to predict runoff during the melt season (Freudiger et al., 2017). Yet, direct mapping of the SWE in mountains remains technologically challenging (Dozier et al., 2016). Recent studies have shown that the assimilation of remotely sensed snow depth data is a viable method for estimating SWE spatial distribution as the SWE can be calculated from the snow depth and the snow density (Brauchli et al., 2017; Margulis et al., 2019; Deschamps-Berger et al., 2022). Efforts are made to address the challenge to map the snow depth in mountainous catchment of societal or ecological interest, typically larger than 100 km² (National Academies of Sciences, Engineering, and Medicine, 2018). Calculating the difference between a snow-on and snow-off digital elevation model (DEM) is one of the most straightforward methods. Snow-on and snow-off DEMs can be derived from airborne lidar or photogrammetry with resolution and vertical precision of 10-30 cm (Deems et al., 2013; Bühler et al., 2015). With the Airborne Snow Observatory

https://doi.org/10.5194/tc-2022-191
Preprint. Discussion started: 4 October 2022

(ASO), several snow dominated catchments of more than 1000 km² are monitored with airborne lidar about every two weeks during the melt-period in California and Colorado, USA. The 3 m resolution snow depth maps have an uncertainty of ~0.1 m (Currier et al., 2019; Mazzotti et al., 2019) and are assimilated in a snowpack model at a lower resolution of 50 m, providing accurate and temporally continuous SWE estimates (Hedrick et al., 2018). However, these flights are expensive, and repeat snow-on flights are only available in a few basins globally. Basins with extensive ASO data are ideal for testing new snow depth detection methods. An alternative to airborne campaigns is to compute DEMs from very-high-resolution stereoscopic satellite images. Snow depth maps at a resolution of 2-3 m were produced from images of the Pléiades or WorldView constellations with an uncertainty of ~0.70 m (Marti et al., 2016; Shaw et al., 2019; McGrath et al., 2019; Deschamps-Berger et al., 2020; Eberhard et al., 2021). The orbits of these satellites enable the imaging of any region of the Earth's surface (cloud-permitting) but the on-demand acquisition mode results in a discontinuous archive in time and space. Snow depth maps have been retrieved from Sentinel-1 observations by calibration with snow depth measurements at automatic weather stations (Lievens et al., 2019; Lievens et al., 2022). A single global calibration factor yielded an error of ~2 m (mean absolute error) at 250 m resolution. With the 12 day revisit of Sentinel-1, this approach provides frequent acquisitions globally at an intermediate spatial resolution. However, this method is not applicable during the melt season when the radar signal is absorbed by the liquid water contained in the snowpack.

Spaceborne lidar missions measure elevation along linear tracks parallel to the satellite orbit. The NASA Ice Cloud and Land Elevation Satellite (ICESat) GLAS instrument was operational from 2003 to 2010 and measured the elevation along a single track every 170 m within a footprint of 70 m. Snow depth could be retrieved from ICESat snow-on observations using a reference airborne lidar snow-off DEM (Treichler et al., 2017). At the footprint scale, the snow depth uncertainty reached an RMSE of 1 m. Due to the sampling structure and the accuracy of ICESat, snow depth data were sparse and not retrieved over slopes greater than 10°. Since October 2018, the higher resolution follow-up mission ICESat-2 has provided improved elevation measurements using ATLAS, a photon-counting lidar instrument. The tracks of ICESat-2 consist of three pairs of a strong and a weak beam with a cross-track distance of 3.3 km between pairs and 90 m between beams. The photon pulses are spaced by ~0.70 m along-track and illuminate an area of ~11 m in diameter (Markus et al., 2017; Smith et al., 2019) with geolocation accuracy of ~3-4 m (Magruder et al., 2021). The individual photon returns are processed to provide estimates of land ice elevation changes with a 20 m spacing along track (ATL06) or forest canopy height at a 100 m spacing (ATL08). Other applications have emerged, including attempts to measure snow depth with ATL08 (Hu et al., 2021). Snow depth was measured with ATL08 data at 16 points with slopes lower than 1.5° and snowpack shallower than 0.35 m. They suggested that this product may not be suitable for rugged topography. We expect ATL06 data to be more relevant to measure snow depth in mountains considering its higher spatial resolution. However, this application is challenging since ICESat-2 was not designed to make frequent repeat measurements at the same locations outside the polar regions. ICESat-2 tracks are offset in the mid-latitudes to increase the spatial density of the point cloud for biomass applications.

Considering the current need to measure snow depth in mountains and the increasing availability of high-precision elevation datasets, we assess the uncertainty of different approaches to retrieve seasonal snow depth from ICESat-2 ATL06 products in

https://doi.org/10.5194/tc-2022-191
Preprint. Discussion started: 4 October 2022

complex terrain. More specifically, we study whether snow depth can be retrieved from ICESat-2 ATL06 measurements only (snow-on and snow-off elevations) or if an additional external DEM is required as a snow-off elevation source. To address these questions, we explored the ICESat-2 ATL06 dataset over the upper Tuolumne basin where airborne snow depth maps are frequently acquired through the ASO program. We obtained over 100,000 snow-on points between October 2018 and November 2021 and compared them with several snow-off elevation sources, including ICESat-2 ATL06 snow-off points, an airborne lidar DEM, a satellite photogrammetry DEM and a satellite InSAR DEM that is globally available (Copernicus DEM). The ICESat-2 ATL06 snow depth retrievals were evaluated against eight airborne lidar snow depth maps from the ASO.

2 Materials and Methods

2.1 ICESat-2 ATL06 elevation product

ATL06 was primarily designed to provide elevation measurements on land ice, yet its coverage extends beyond glacier areas such that sparse ATL06 data are available even in ranges with very limited glacier cover such as the Sierra Nevada (Smith et al., 2019). The ATL06 product is produced by fitting 40 m segments to the land-surface photon returns along each of the six tracks, with segments overlapping by 20 m. The mean surface height of each segment is provided as point data positioned at the center of that segment and is labeled h_mean in the ATL06 data product (Smith et al., 2019). The overlap of the segments results in a point located every 20 m along-track for each of the six tracks.

The upper Tuolumne river basin spans an elevation range of 1200 m to 4200 m and consists of 1100 km² montane forests and alpine zones. All available ATL06 granules result in 265,590 points intersecting the basin and spanning from 15 October 2018 to 7 November 2021. 4% of the points were discarded since their elevation value was non valid (no data) or their error was large (sigma_h_mean > 1000 m). The number of photons (n_fit_photons) used to calculate the height of each point is variable as snow and ice are highly reflective in the ATLAS beam wavelength (532 nm). We classified snow as present when the number of photon returns exceeded a certain threshold (Figure 2 and S1). This threshold was determined by comparing the number of photons with MODIS snow cover observations. A daily stack of snow cover maps was generated by linear interpolation of the MOD10A1 "NDSI_Snow_Cover" in the time dimension on a pixel basis. The resulting gap-free time series of NDSI layers was binarized to snow and no-snow maps using a NDSI threshold of 0.2. Cohen's kappa was used as the objective function to maximize to find the optimal number of photons (Cohen, 1969; Gascoin et al., 2015).

2.2 Snow-off elevation data

We used four snow-off DEMs from ICESat-2 ATL06 itself, airborne lidar, satellite photogrammetry and satellite InSAR as explained below (Table 1).

(i) We generated the ICESat-2 snow-off DEM at 15 m resolution from all snow-off points using a gaussian weighted interpolation with a search radius of half a pixel with the point2dem utility of the Ames Stereo Pipeline (Shean et al., 2016; Beyer et al., 2018). Here, we assumed that each ATL06 point corresponds to a pixel of 15 m by 15 m.

https://doi.org/10.5194/tc-2022-191
Preprint. Discussion started: 4 October 2022

(ii) A Digital terrain model (DTM) at 3 m grid spacing was measured with airborne lidar during the ASO campaign on 13 October 2015 (Painter et al., 2016).

(iii) A DEM at 3 m grid spacing was calculated from stereographic images of the satellite Pléiades on 13 August 2017 (Deschamps-Berger et al., 2020). This DEM covers 220 km² of the upper Tuolumne basin (i.e. 20% of the total area).

(iv) A DEM from the Copernicus-30 global dataset was extracted at its native grid spacing of 30 m. The Copernicus-30 product is derived from InSAR data of the TanDEM-X mission in most areas with some areas filled with miscellaneous external products.

Consistent spatial resolution between the snow-off and snow-on products is expected to improve the derived snow depth. However, the exact spatial scale of the ATL06 points remains uncertain. The maximum sampling area of each ATL06 point is 40 m (i.e. the segment length) by ~11 m (i.e. the footprint width). However the extraction of the elevation at the center of a linear segment fitted through the photons might represent the elevation at a finer scale. Thus, the Pléiades and ASO DEMs were used at their native resolution (3 m) but also at a coarser resolution of 15 m (resampling by averaging the contributing pixels) to allow an evaluation of the true scale of ATL06 points. The Copernicus DEM was left at its native 30 m resolution.

All DEMs, except the ICESat-2 snow-off DEM, were co-registered to the ICESat-2 snow-off point cloud using Nuth and Kääb (2011) method. This method relates the horizontal co-registration vector between two elevation datasets with the elevation difference between the two datasets, the slope and the aspect of the terrain. It can be used with gridded product (e.g. lidar or photogrammetry DEM) or irregularly distributed points (e.g. ICESat-2 ATL06). The elevation of the DEM is extracted at the ICESat-2 point position with a spline linear interpolation scheme (scipy.interpolate.interp2d). The slope and aspect are calculated from the DEM and extracted with the same method. The slopes steeper than 45° (i.e. prone to error in the elevation dataset) and smaller than 10° (i.e. which lead to a divergence of the Nuth and Kääb (2011) equation) are excluded. A co-registration vector is iteratively calculated and applied to the DEM, the aspect and the slope raster. The iteration stops when the co-registration vector is shorter than 0.1 m or when the normalized median absolute deviation (NMAD, i.e. error metric) of the elevation difference is improved by less than 1%. After the horizontal co-registration vector is applied, a vertical shift is applied based on the mode of the elevation residual distribution (Table S1).

Due to the difference in structure between the gridded snow-off DEM and the ICESat-2 snow-on points, the elevation of the snow-off DEMs had to be interpolated linearly at each ICESat-2 snow-on point to calculate the "ICESat-2 derived snow depth". For the ICESat-2 snow-off DEM, the elevation was extracted at the snow-on point by nearest-neighbor interpolation as the snow-off DEM was too sparse to use a linear interpolation of neighboring pixels. The ICESat-2 derived snow depth products were labeled after the snow-off DEM source and resolution, e.g. "IS2-ASO 3 m" refers to the snow depth computed as the difference between ICESat-2 (IS2) snow-on points and ASO snow-off DEM at 3 m resolution (Table S2).

https://doi.org/10.5194/tc-2022-191
Preprint. Discussion started: 4 October 2022

Table 1. Elevation and snow depth dataset used in this study.

Data	Source	Structure	Spatial resolution	Date
Elevation points	ICESat-2 ATL06	Points	20 m	2018-10-15 to 2021-11-07
Digital Terrain Model	Airborne lidar (ASO)	Regular grid	3 m	2015-10-13
Digital Surface Model	Satellite photogrammetry (Pléiades)	Regular grid	3 m	2017-08-13
Digital Surface Model	Copernicus DEM – 30 m	Regular grid	30 m	-
Snow depth map	Airborne lidar (ASO)	Regular grid	3 m	2019-03-24 2019-04-17 2019-05-03 2019-07-05 2020-04-13 2020-05-07 2020-05-22 2021-04-29

2.3 Evaluation of the snow depths

Eight snow depth maps at 3 m grid spacing from the ASO program were available at different dates over the study period (Table 1). The maps were shifted horizontally according to the vector used to co-register the ASO DTM to the ICESat-2 snow-off points. The ASO snow depth maps were used at their native resolution and were also resampled by averaging at 15 m to evaluate the scale of ATL06 points. For each ICESat-2 derived snow depth, the snow depth value of the closest ASO snow depth map in time was extracted. We use the term accuracy to describe biases in snow depth while precision is used for random errors (Hugonnet et al., 2022). The accuracy of the ICESat-2 derived snow depths was evaluated with the median of the residual (e.g. IS2-ASO 3 m snow depth minus ASO snow depth) while the precision was evaluated with the Normalized Median Absolute Deviation of the residual (NMAD, Höhle and Höhle, 2009), a measure of dispersion robust to outliers.

The uncertainty of airborne and satellite laser elevations increases when the slope increases as steep slopes spread the photons return timing compared to flat terrain (Deems et al., 2013; Treichler et al., 2017). We evaluate the impact of slopes on ICESat-2 derived snow-depth thanks to slope maps derived from the ASO DTM at 3 m and 15 m. Vegetation (bushes, isolated trees, forests) is also expected to impact the accuracy and precision of the ICESat-2 derived snow depths as vegetation is handled differently in each elevation source. The ICESat-2 ATL06 points were produced without explicitly excluding the photons reflected by the vegetation, thus including photons from the top of the canopy to the ground. The ASO DEM is a DTM, i.e. the ground surface is measured with vegetation excluded. The Pléiades DEM measures the visible

https://doi.org/10.5194/tc-2022-191
Preprint. Discussion started: 4 October 2022

surface of the vegetation, i.e. a digital surface model. Therefore, the impact of the vegetation on the ICESat-2 derived snow depths was also evaluated using the tree cover density at each point position from the Landsat-MODIS 30 m product (Sexton et al., 2013).

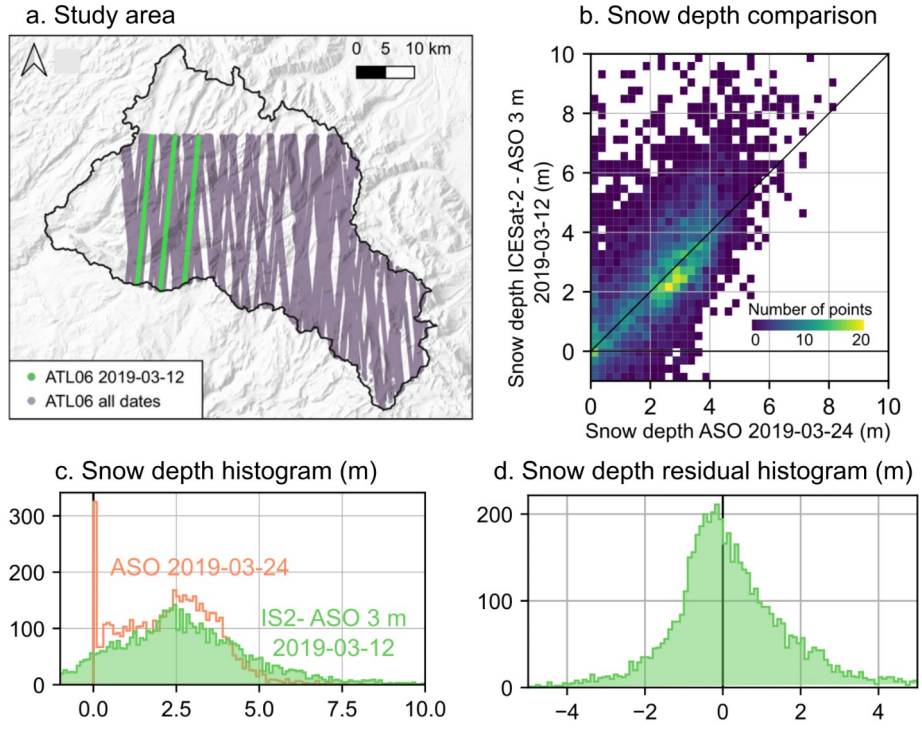

Figure 1. The upper Tuolumne basin (a) and all the ICESat-2 ATL06 points available (purple) between October 2018 and November 2021, with the 12 March 2019 track highlighted (green). Heat-map (b) and general distribution (c) of the ICESat-2-ASO 3 m snow depth on 12 March 2019 (green) and airborne lidar snow depth twelve days later (orange). Histogram of the snow depth residual (d).

3 Results

3.1 Spatial and temporal data availability

Figure 1a shows the 255,802 ATL06 points available over the 1100 km² of the upper Tuolumne river basin between 15 October 2018 and 7 November 2021. The number of photon returned for each ATL06 point varies seasonally and is lowest from June to October during the snow-free season (Figure 2). The optimization of the photon count threshold is robust (Figure S1) with 50 photons for the weak beam points and 186 photons for the strong beam points. With these thresholds, 59% of the points were classified as snow-off. This results in a sparse ICESat-2 snow-off DEM with 25 km² of valid data on a grid of 15 m resolution, which is 2% of the basin (Figure 3), since many pixels were not intersected by an ATL06 point. The remaining snow-on points were distributed on 50 dates with half of the dates containing less than 700 points and the remaining dates with more, up to 8000 points, which means at best a coverage of 1.8 km² if gridding the points on a 15 m

https://doi.org/10.5194/tc-2022-191
Preprint. Discussion started: 4 October 2022

grid (Figure 1a). About half of the points were in areas with a low tree cover density (< 10%) of which 45% were snow-covered. Some points were obtained in areas with higher tree cover density up to 70%, close to the maximum observed in the upper Tuolumne basin (72%).

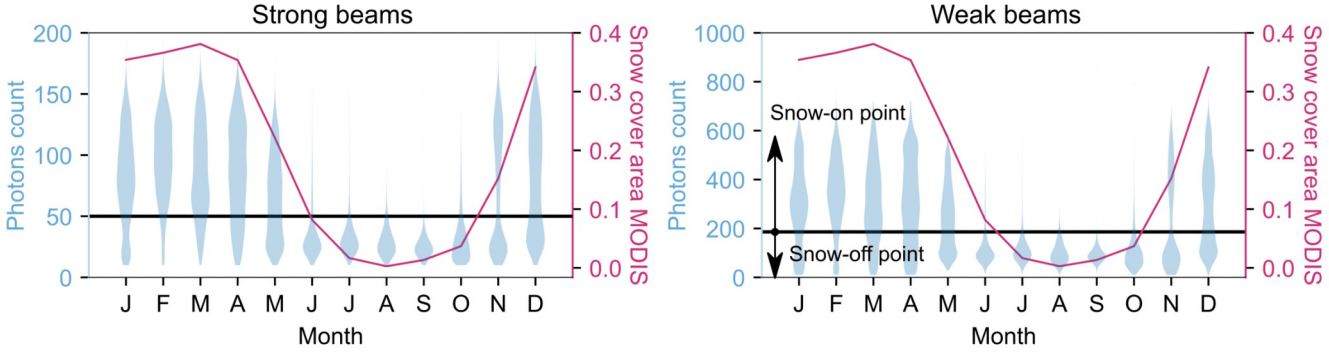

Figure 2. Distribution of photons counts by beam and month for ICESat-2 ATL06 points. ICESat-2 has three pairs of beams. Each beam of a pair is either strong or weak depending on the number of photons per pulse. The photon count thresholds to determine snow-on and snow-off points optimized with MODIS snow cover area are marked by a black line. The monthly mean snow cover area from MODIS over the period is in red.

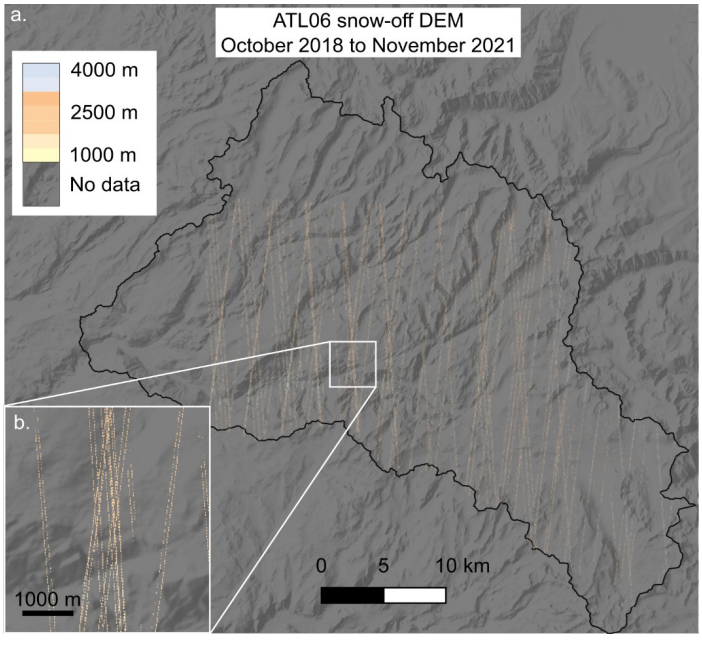

Figure 3. Snow-off DEM from ICESat-2 ATL06 points classified as without snow collected between October 2018 and November 2021 gridded on a 15 m grid. The DEM is sparse and only provides 25 km² of valid data in the 1100 km² upper Tuolumne basin.

3.2 Impact of the snow-off DEM source

https://doi.org/10.5194/tc-2022-191
Preprint. Discussion started: 4 October 2022

Few snow-on points intersected the ICESat-2 ATL06 snow-off DEM, due to its sparse coverage (Figure 3). The other gridded external DEMs provided over 10 times more snow depth points due to their higher incidence of overlap with ATL06 snow-on points. In the next sections we present results for 12 March 2019 as it is the only date with snow-on points covering a large range of snow depth, which intersect the Pléiades snow-off DEM coverage and with an ASO snow depth map acquired only 12 days later. The snowpack changed a little as the Lower Kibbie Ridge station (2042 m a.s.l., within the basin) measured +0.01 m water equivalent (w.e.) accumulation between the IS2 track (12 March) and the ASO snow depth map (24 March) (SNOTEL data).

On 12 March 2019, we obtained the best results from the combination of ICESat-2 ATL06 and ASO 3 m snow-off DEM (IS2-ASO 3 m) and ICESat-2 ATL06 and Pléiades 3 m snow-off DEM (IS2-Pléiades 3 m) (Figure 1, 4, Table S2). The ICESat-2 derived snow depth have a low bias of 0.04 m (median IS2-ASO 3 m) and -0.17 m (median IS2-Pléiades 3 m), and a precision of 1.19 m (NMAD IS2-ASO 3 m) and 1.11 m (NMAD IS2-Pléiades 3 m). More points were available for IS2-ASO 3 m (N=5450) than IS2-Pléiades 3 m (N=1295), making the evaluation more robust for the former. The 127 snow depths available for IS2-IS2 15 m had a larger bias (median=-1.03 m) and worse precision (NMAD=3.63 m). The IS2-Copernicus 30 m snow depths showed the worst accuracy (median=-1.09 m) and precision (NMAD=10.92 m) (Table S2). Thus, we disqualified the IS2-Copernicus 30 m snow depths and excluded it from the following analysis (Figure S2 and S3).

The other dates mirror the accuracy and precision found on 12 March 2019 (Figure 4 g, h, i), with the exception of the precision of IS2-Pléiades 3 m which were degraded on 15 July 2019 (NMAD=1.57 m) and 10 May 2021 (NMAD=1.55 m). The median bias of IS2-ASO 3 m is smaller in absolute than 0.15 m for five dates and between -0.26 m and -0.58 m for the three other dates. The IS2-IS2 15 m might be better evaluated on 14 May 2019 where snow-off and snow-on tracks were nearly colocated, providing 2760 snow depth points. On that date, the precision was better (NMAD=1.65 m) than on 12 March 2019 (NMAD=3.63 m) but the accuracy was worse (median=-0.85 m). This is likely a result of actual snow depth change as the Lower Kibbie Ridge station measured 0.28 m w.e. ablation between the ASO snow depth map (3 May) and the IS2 track (15 May).

3.3 Impact of the terrain slope

ICESat-2 derived snow depth showed a general better agreement with ASO snow depth in areas with low slopes (Figure 4 a, b). For slopes below 10°, IS2-ASO 3 m and IS2-Pléiades 3 m had a similar precision with a NMAD of, respectively, 0.51 m and 0.76 m. The precision was worse for IS2-IS2 15 m (NMAD=1.68 m). The accuracy for this range of slopes was similar for all products (i.e. median between -0.27 m and -0.36 m). Note that the co-registration corrected the vertical bias on all points with slopes up to 45° and cannot ensure a lack of bias for any subset of slopes (e.g. slopes between 0° and 10°).

IS2-ASO 3 m snow depths precision and accuracy worsened with increasing slope. The median residual increased gradually from -0.36 m for slopes between 0° and 10° to +0.73 m for slopes between 30° and 40°. Over the same range of slopes, the precision decreased as well with the NMAD growing from 0.38 m to 1.38 m. The NMAD of IS2-Pléiades 3 m grew comparatively less, from 0.81 m to 1.30 m for the same slopes.

https://doi.org/10.5194/tc-2022-191
Preprint. Discussion started: 4 October 2022

210 **3.4 Impact of the vegetation density**

The IS2-ASO 3 m snow depth accuracy and precision were roughly constant up to 60% of tree cover density, i.e. the maximum sampled by the 12 March 2019 tracks (Figure 4 c, d). This suggests that ICESat-2 ATL06 points captured the surface elevation below the canopy in this area despite the vegetation. However, the distribution of the elevation difference between ICESat-2 snow-off points and ASO DTM was positively skewed (not shown), suggesting that vegetation partly led
215 to an overestimation of the ground elevation for snow-off ATL06 points. Acknowledging this, we used the mode of the residual distribution to vertically co-register the ASO DTM. Using the median, i.e. as often done (Deschamps-Berger et al., 2020; Shean et al., 2020), would increase the snow depth bias by 0.54 m. The IS2-Pléiades 3 m snow depth was sensitive to the tree density with a decrease in precision and a strong negative bias for tree cover density between 30% and 40% (median=-1.52 m) and between 40% and 50% (median= -4.12 m).

220

3.5 Scale of the ICESat-2 ATL06 measurements and impact of the beams and of the elevation retrieval algorithm

The 15 m snow depth retrievals were mostly as accurate and precise as the 3 m retrievals for the ASO and Pléiades snow-off DEMs (Figure 4). For IS2-IS2 15 m evaluation, only the resolution of the ASO reference snow depth maps were modified since higher resolution cannot be obtained for the IS2 snow-off DEM due to the 20 m spacing of the ATL06 points. The
225 modification of the snow depth map resolution did not impact the accuracy estimation of the IS2-IS2 15 m.

We repeated the same workflow only using ATL06 elevations corrected for the first-photon bias and the transmit-pulse-shape error (h_li) instead of the linear fit at the center of the segment (h_mean). The snow depth products were very similar for both algorithms (Figure S4). Considering separately the snow-on point of the strong or the weak beam yield slightly larger uncertainty for the strong beam on the steep slopes and smaller uncertainties in forested area (Figure S5 and S6).

230

https://doi.org/10.5194/tc-2022-191
Preprint. Discussion started: 4 October 2022

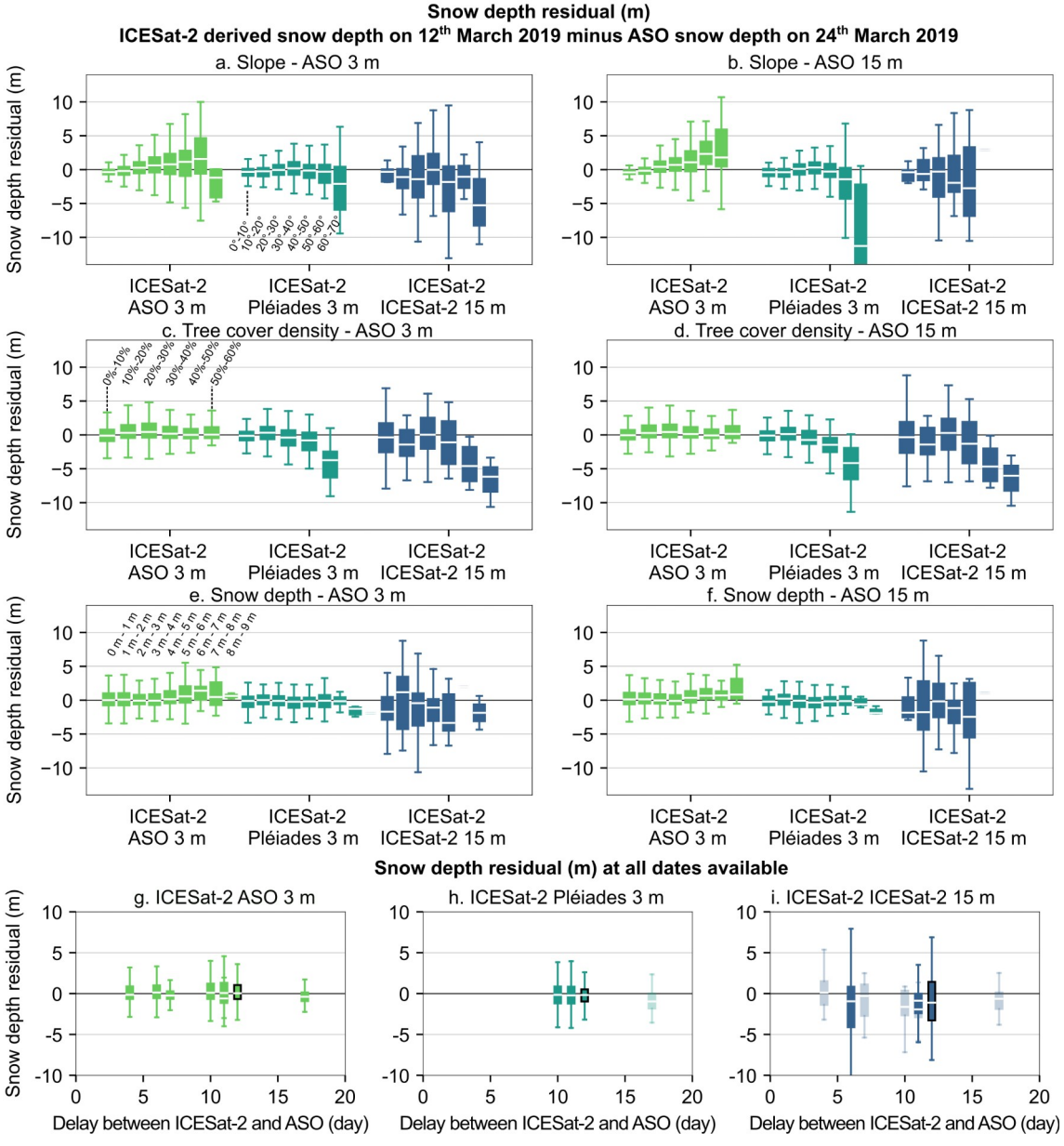

Figure 4. Snow depth residuals (ICESat-2 derived snow depth minus ASO snow depth). Each group of boxplots (or color) corresponds to a snow-off DEM. Within each group, the boxplots are classified by terrain slope (a, b), tree cover density (c, d) and snow depth (e, f). The residuals were calculated from the product at their native resolution (a, c, e) or averaged at 15 m for ASO DEM, Pléiades DEM and ASO snow depth (b, d, f). The snow depth derived from ICESat-2 and ASO 3 m DEM are the most accurate and precise for all tree cover densities. The snow depth retrieved from ICESat-2 and Pléiades 3 m DEM have a similar precision for open or flat terrain but a better for steeper slopes. Snow depth residuals when an ASO snow depth map is available

https://doi.org/10.5194/tc-2022-191
Preprint. Discussion started: 4 October 2022


The Cryosphere Discussions

at less than 20 days (g, h, i). Transparent boxplots show the dates where less than 100 points were available. The black boxplot is the residual on 12 March 2019 shown in upper panels. Higher temporal resolution and more points per date are available using gridded DEMs with full coverage of the study area (g, h). The best precision and accuracy is obtained with the ASO DEM (g) and the Pléiades DEM (h).

4 Discussion

The snow depth retrieved from ICESat-2 ATL06 data only (IS2-IS2 15 m) might not prove useful to many applications in terms of temporal and spatial availability. The ICESat-2 snow-free DEM coverage is currently sparse, but is expected to improve over time as new tracks are acquired by the satellite at these latitudes. The retrieval of the IS2-IS2 15 m snow depth through nearest-neighbor interpolation is suboptimal as it does not take into account the variation of the terrain. Better results are expected if a linear or cubic interpolation at the intersection between the snow-off and the snow-on track is conducted.

Using an external DEM as a snow-off reference improves the data coverage and allows the use of every ICESat-2 snow-on point. The best results were obtained with the airborne lidar DEM and the satellite photogrammetry DEM (e.g. IS2-ASO 3 m, IS2-Pléiades 3 m). The airborne lidar DTM measures the ground surface below the tree canopy and ensures ICESat-2 snow depth retrieval even in forest with density up to 60%. Airborne lidar datasets are increasingly freely available in parts of the world (e.g. in Northern America and Europe). Yet, the vast majority of the world's mountains remain uncharted. Our results suggest that using a satellite photogrammetry snow-off DEM is a viable alternative as it provides snow depth with a similar accuracy to airborne lidar for tree cover density below 30% and even a better estimation of snow depth in steep slopes. High-resolution DEM from satellite photogrammetry are already available in the Arctic (Porter et al., 2018), the Antarctic (Howat et al., 2019) and the Himalayas (Shean, 2017). However, the time stamp is not provided in the mosaiced products and this might hinder the identification of the snow-off from the snow-on pixels. In other areas, images from the Pléiades, World-View or the Planet-SkySat satellites can be acquired on-demand to generate a snow-off DEM. The Copernicus-30 DEM has a global coverage but its coarse resolution seems to be disqualifying for this application partly because it hampers an accurate co-registration. The co-registration is considered successful for the ASO snow-off DEM and the Pléiades DEM considering the decrease of the error metric over the stable terrain (Table S1). The residual elevation difference between both DEMs is close to 0 m on low slope and increases up to ~1 m for steeper slopes (Figure S2 b). This matches the comparison of the two DEMs when they are co-registered together (Figure S2 in Deschamps-Berger et al., 2020). However, the precision of the *IS2-Copernicus 30 m* snow depths was improved when the Copernicus DEM was co-registered to the ASO DEM (NMAD=7.03 m) rather than to the ICESat-2 snow-off points (NMAD=10.92 m) (Figure S2 and S3). This approach could not be applied in the general case as an accurate airborne lidar DEM is needed. The Copernicus 10 m product might have sufficient accuracy to derive snow depth but is only available over Europe.

The snow depths derived here from ICESat-2 ATL06 are more accurate, have a finer spatial scale and a denser spatial coverage than snow depths derived with a similar approach from ICESat products (Treichler and Kääb, 2017). ICESat derived snow depths had an RMSE of 1 m over slopes lower than 10° at the 70 m footprint scale (N=27) and steeper slopes

https://doi.org/10.5194/tc-2022-191
Preprint. Discussion started: 4 October 2022

were excluded as prone to large errors in ICESat. Here, we obtained an RMSE of 0.85 m (N=907) over slopes lower than 10° on 12 March 2019 at a 3 m scale (IS2-ASO 3 m). The progressive degradation of the accuracy with the increasing slope was also characterized and found to be less pronounced for IS2-Pléiades 3 m than IS2-ASO 3 m. The rough and vegetated mountain terrain of our study site, as expected, degrades ATL06 accuracy. ATL06 elevations were ten times more accurate over the Antarctic ice sheet than the elevation difference evaluated in this study with a precision of 0.09 m (standard deviation) compared to GNSS measurements (Brunt et al., 2019). The calculation of ATL06 elevation from ATL03 products was optimized for glaciers and ice sheets which often have flat and smooth surfaces. Improved precision might be obtained by adapting this processing to mountainous terrain (Shean et al., 2022).

The ICESat-2 ATL06 snow depth (NMAD between 0.5 m and 1.2 m) are less precise than snow depths derived from airborne lidar only (Mazzotti et al., 2019) and similar or slightly worse than what is obtained with satellite photogrammetry only (Eberhard et al., 2021, Deschamps-Berger et al., 2020). In terms of relative error, the snow depth shows a typical error of 40% or less for snow depth thicker than 2 m and larger errors for shallower snowpack (Figure S7). This is comparable to the error of snow depth retrieved from Sentinel-1 (Lievens et al., 2022). Thus, the existing approaches combining satellite photogrammetry or Sentinel-1 snow depth with snowpack models (e.g. assimilation) should be appropriate for ICESat-2 derived snow depth (Shaw et al., 2020, Deschamps-Berger et al., 2022, Alfieri et al., 2021). However, ICESat-2's variable temporal resolution and sparse transect data is unique compared to spatially continuous airborne or satellite maps and gridded snow model results. Figure S8 shows the inter-annual variability of the snow depth gradient with elevation measured by the ICESat-2 track. The ICESat-2 track only covers parts of the elevation with snow cover, and the snow depth distribution differs in both dataset over the sampled altitudes. Only relying on sparse ICESat-2 derived snow depths would lead to an inaccurate estimation of the snow volume of the basin. One promising approach to utilizing ICESat-2-derived snow depth transects comes from Pflug and Lundquist (2020), where snow patterns in the upper Tuolumne basin were shown to be repeating and scalable. Small strips of snow depths were matched with a library of distributed snow depth maps from prior years to produce distributed snow depth maps of the basin. An ICESat-2 track might be used in this way to represent a relevant subset of a basin.

Each ICESat-2 ATL06 snow depth point is informative over a small sampling area as the snow depth seems as representative of 3 m pixels as of 15 m pixels (Figure 4). The good quality of snow depth derived from ATL06 at this fine scale suggests that ATL03 products might provide finer scale and spatially richer snow depth, as each photon returned to ICESat-2 is provided in this product.

6 Conclusion

The retrieval of snow depth from ICESat-2 ATL06 data only is currently limited by the coverage of the ATL06 snow-off points, but the point density will increase as long as the ICESat-2 mission continues. However, ICESat-2 ATL06 snow-on elevation combined with airborne lidar or satellite photogrammetry snow-off DEMs is a promising way to measure accurate snow depth at high-resolution in mountains. We found that little filtering of the ALT06 points was required and that a single

co-registration of the snow-off DEM was sufficient. The photon counts variable provided with ATL06 points can be used to classify snow-on and snow-off points. It remains uncertain whether the threshold found here could be transferred in regions with different vegetation cover, terrain roughness and cloudiness. By combining ICESat-2 snow-on points with an airborne lidar or satellite photogrammetry DEM, a precision of ~1.2 m and a bias of ~0.2 m is obtained for a typical mountain environment, i.e. which includes snow depths up to 8 m and a large range of slope. As expected, increasing slope degrades the snow depth retrieval while tree cover mostly degrades ICESat-2 products combined with a digital surface model (i.e. satellite photogrammetry). Given the promising results reported here, we believe that the generation of ATL06 products over non-glacierized mountainous regions is desirable to help with water resources estimation in unmonitored mountains.

Author contribution

CDB and SG designed the study. AG performed the initial data curation under and formal analysis further led by CDB and SG. DS and HB contributed to the methodology and the validation of the results. All authors contributed to writing the manuscript. SG and NLM ensured the funding acquisition.

The authors declare that they have no conflict of interest.

Acknowledgments

This work has been supported by the Programme National de Télédétection Spatiale (PNTS; grant no. PNTS-2018-4). SG is supported by CNES. AG was supported by Météo-France during the internship which laid the groundwork of this article. We thank Etienne Berthier for reading an advanced version of the manuscript and providing helpful suggestions.

Open Research

ICESat-2 ATL06 data were downloaded from https://nsidc.org/data/ATL06/versions/5 on 1 March 2022

ASO snow depth maps and digital surface model were downloaded from https://nsidc.org/data/ASO_3M_SD/versions/1 and https://data.airbornesnowobservatories.com/#

The Pléiades DEM is available at https://zenodo.org/record/6466891#.Yl0SuNPP02w

Copernicus 30 m DEM was downloaded from https://spacedata.copernicus.eu/web/cscda/data-access

Code is available at https://framagit.org/cesardb/icesat-2-mapping-of-snow-height.git

References

Alfieri, L., Avanzi, F., Delogu, F., Gabellani, S., Bruno, G., Campo, L., Libertino, A., Massari, C., Trapanelli, A., Rains, D., Miralles, D. G., Quast, R., Vreugdenhil, M., Wu, H., and Brocca, L.: High resolution satellite products improve hydrological modeling in northern Italy, Hydrology and Earth System Sciences Discussions, December, 1–29, doi.org/10.5194/hess-26-3921-2022, 2021.

Barnett, T. P., Adam, J. C., and Lettenmaier, D. P.: Potential impacts of a warming climate on water availability in snow-dominated regions, Nature, 438(7066):303–309, doi.org/10.1038/nature04141, 2005.

Beyer, R. A., Alexandrov, O., and Scott, M.: The Ames Stereo Pipeline: NASA's Open Source Software for Deriving and Processing Terrain Data Special Section, Earth and Space Science, 5:537–548, doi.org/10.1029/2018EA000409, 2018.

Brauchli, T., Trujillo, E., Huwald, H., and Lehning, M.: Influence of Slope-Scale Snowmelt on Catchment Response Simulated With the Alpine3D Model, Water Resources Research, 1–17, doi.org/10.1002/2017WR021278, 2017.

Cohen, J.: A coefficient of agreement for nominal scales, Educ. Psychol. Meas., 20, 37–46, 1960.

Currier, W. R., Pflug, J., Mazzotti, G., Jonas, T., Deems, J. S., Bormann, K. J., Painter, T. H., Hiemstra, C. A., Gelvin, A., Uhlmann, Z., Spaete, L., Glenn, N. F., and Lundquist, J. D.: Comparing Aerial Lidar Observations With Terrestrial Lidar and Snow-Probe Transects From NASA's 2017 SnowEx Campaign, Water Resources Research, 55(7), 6285–6294. doi.org/10.1029/2018WR024533, 2019.

Deems, J. S., Painter, T. H., and Finnegan, D. C. (2013). Lidar measurement of snow depth : a review. Journal of Glaciology, 59(215):467–479, doi.org/10.3189/2013JoG12J154, 2013.

Deschamps-Berger, C., Cluzet, B., Dumont, M., Lafaysse, M., Berthier, E., Fanise, P., and Gascoin, S.: Improving the spatial distribution of snow cover simulations by assimilation of satellite stereoscopic imagery, Water Resources Research, 58(3), doi.org/10.1029/2021WR030271, 2022.

Deschamps-Berger, C., Gascoin, S., Berthier, E., Deems, J., Gutmann, E., Dehecq, E., Shean, D., and Dumont, M.: Snow depth mapping from stereo satellite imagery in mountainous terrain: evaluation using airborne lidar data. The Cryosphere, (February):1–28, doi.org/10.5194/tc-14-2925-2020, 2020.

Dozier, J., Bair, E. H., and Davis, R. E.: Estimating the spatial distribution of snow water equivalent in the world's mountains, Wiley Interdisciplinary Reviews: Water, 3(3), 461–474. doi.org/10.1002/wat2.1140, 2016.

Eberhard, L. A., Sirguey, P., Miller, A., Marty, M., Schindler, K., Stoffel, A., and Bühler, Y.: Intercomparison of photogrammetric platforms for spatially continuous snow depth mapping, The Cryosphere, 15, 69–94, doi.org/10.5194/tc-15-69-2021, 2021.

Freudiger, D., Kohn, I., Seibert, J., Stahl, K., and Weiler, M.: Snow redistribution for the hydrological modeling of alpine catchments, Wiley Interdisciplinary Reviews: Water, pages 1–16, doi.org/10.1002/wat2.1232, 2017.

Gascoin, S., Hagolle, O., Huc, M., Jarlan, L., Dejoux, J. F., Szczypta, C., Marti, R., and Sánchez, R.: A snow cover climatology for the Pyrenees from MODIS snow products, Hydrology and Earth System Sciences, 19(5), 2337–2351, doi.org/10.5194/hess-19-2337-2015, 2015.

Hedrick, A., Marks, D., Havens, S., Robertson, M., Johnson, M., Micah, S., Marshall, H.-P., Kormos, P. R., Bormann, K. J., and Painter, T. H.: Direct Insertion of NASA Airborne Snow Observatory Derived Snow Depth Time Series Into the iSnobal Energy Balance Snow Model, Water Resources Research, 54:8045–8063, doi.org/10.1029/2018WR023190, 2018.

Höhle, J. and Höhle, M.: Accuracy assessment of digital elevation models by means of robust statistical methods, ISPRS Journal of Photogrammetry and Remote Sensing, 64(4):398–406, doi.org/10.1016/j.isprsjprs.2009.02.003, 2009.

Howat, I. M., Porter, C., Smith, B. E., Noh, M.-J., and Morin, P.: The Reference Elevation Model of Antarctica, The Cryosphere, 13, 665-674, doi.org/10.5194/tc-13-665-2019, 2019.

Hu, X., Hao, X., Wang, J., Huang, G., Li, H., and Yang, Q.: Can the Depth of Seasonal Snow be Estimated from ICESat-2 Products: A Case Investigation in Altay, Northwest China, IEEE Geoscience and Remote Sensing Letters, 19:1–5, doi.org/10.1109/LGRS.2021.3078805, 2021.

Hugonnet, R., Brun, F., Berthier, E., Dehecq, A., Mannerfelt, S., Eckert, N., Farinotti, D.: Uncertainty analysis of digital elevation models by spatial inference from stable terrain, IEEE Journal of Selected Topics in Applied Earth Observations and Remote Sensing, 1–17, doi.org/10.1109/JSTARS.2022.3188922, 2022.

Lievens, H., Brangers, I., Marshall, H. P., Jonas, T., Olefs, M., and De Lannoy, G.: Sentinel-1 snow depth retrieval at sub-kilometer resolution over the European Alps, The Cryosphere, 16(1):159–177, doi.org/10.5194/tc-16-159-2022, 2022.

Lievens, H., Demuzere, M., Marshall, H. P., Reichle,R. H., Brucker, L., Brangers, I., Rosnay, P. D., Dumont, M., Girotto, M., Immerzeel, W. W., Jonas, T., Kim, E. J., Koch, I., Marty, C., Saloranta, T., Schöber, J., and De Lannoy, G. J. M.: Snow depth variability in the Northern Hemisphere mountains observed from space, Nature Communications, 1–12, doi.org/10.1038/s41467-019-12566-y, 2019.

Magruder, L., Brunt, K., Neumann, T., Klotz, B., and Alonzo, M.: Passive Ground-Based Optical Techniques for Monitoring the On-Orbit ICESat-2 Altimeter Geolocation and Footprint Diameter, Earth and Space Science, 8(10):1–9, doi.org/10.1029/2020EA001414, 2021.

Margulis, S. A., Fang, Y., Li, D., Lettenmaier, D. P., and Andreadis, K.: The utility of infrequent snow depth images for deriving continuous space-time estimates of seasonal snow water equivalent, Geophysical Research Letters, 46, doi.org/10.1029/2019GL082507, 2019.

Markus, T., Neumann, T., Martino, A., Abdalati, W., Brunt, K., Csatho, B., Farrell, S., Fricker, H., Gardner, A., Harding, D., Jasinski, M., Kwok, R., Magruder, L., Lubin, D., Luthcke, S., Morison, J., Nelson, R., Neuenschwander, A., Palm, S., Popescu, S., Shum, C. K., Schutz, B. E., Smith, B., Yang, Y., and Zwally, J.: The Ice, Cloud, and land Elevation Satellite-2 (ICESat-2): Science requirements, concept, and implementation, Remote Sensing of Environment, 190:260–273, doi.org/10.1016/j.rse.2016.12.029 , 2017.

Marti, R., Gascoin, S., Berthier, E., De Pinel, M., Houet, T., and Laffly, D.: Mapping snow depth in open alpine terrain from stereo satellite imagery, The Cryosphere, 10(4):1361–1380, doi.org/10.5194/tc-10-1361-2016, 2016.

Mazzotti, G., Currier, W. R., Deems, J. S., Pflug, J. M., Lundquist, J. D., and Jonas, T.: Revisiting Snow Cover Variability and Canopy Structure Within Forest Stands: Insights From Airborne Lidar Data, Water Resources Research, 55(7), 6198–6216, doi.org/10.1029/2019WR024898, 2019.

https://doi.org/10.5194/tc-2022-191
Preprint. Discussion started: 4 October 2022

McGrath, D., Webb, R., Shean, D., Bonnell, R., and Marshall, H. P.: Spatially Extensive Ground-Penetrating Radar Snow Depth Observations During NASA's 2017 SnowEx Campaign : Comparison With In Situ , Airborne , and Satellite Observations Water Resources Research. Water Resources Research, 10, doi.org/10.1029/2019WR024907, 2019.

National Academies of Sciences, Engineering, and Medicine: Thriving on Our Changing Planet: A Decadal Strategy for Earth Observation from Space. Washington, DC: The National Academies Press. Appendix C., doi.org/10.17226/24938, 2018.

Painter, T. H., Berisford, D. F., Boardman, J. W., Bormann, K. J., Deems, J. S., Gehrke, F., Hedrick, A., Joyce, M., Laidlaw, R., Marks, D., Mattmann, C., McGurk, B., Ramirez, P., Richardson, M., Skiles, S. M. K., Seidel, F. C., and Winstral, A.: The Airborne Snow Observatory: Fusion of scanning lidar, imaging spectrometer, and physically-based modeling for mapping snow water equivalent and snow albedo, Remote Sensing of Environment, 184:139–152, doi.org/10.1016/j.rse.2016.06.018, 2016.

Pflug, J. M. and Lundquist, J. D.: Inferring Distributed Snow Depth by Leveraging Snow Pattern Repeatability: Investigation Using 47 Lidar Observations in the Tuolumne Watershed , Sierra Nevada , California, Water Resources Research, 56, doi.org/10.1029/2020WR027243, 2020.

Porter, C., Morin, P., Howat, I., Noh, M.-J., Bates, B., Peterman, K., Keesey, S., Schlenk, M., Gardiner, J., Tomko, K., Willis, M., Kelleher, C., Cloutier, M., Husby, E., Foga, S., Nakamura, H., Platson, M., Wethington, M., Williamson, C., Bauer, G., Enos, J., Arnold, G., Kramer, W., Becker, P., Doshi, A., D'Souza, C., Cummens, P., Laurier, F., Bojesen, M.: "ArcticDEM", doi.org/10.7910/DVN/OHHUKH, Harvard Dataverse, V1, 2018.

Sexton, J. O., Song, X. P., Feng, M., Noojipady, P., Anand, A., Huang, C., Kim, D. H., Collins, K. M., Channan, S., DiMiceli, C., and Townshend, J. R.: Global, 30-m resolution continuous fields of tree cover: Landsat-based rescaling of MODIS vegetation continuous fields with lidar-based estimates of error, International Journal of Digital Earth, 6(5):427–448, doi.org/10.1080/17538947.2013.786146, 2013.

Shaw, T. E., Gascoin, S., Mendoza, P. A., Pellicciotti, F., and McPhee, J.: Snow depth patterns in a high mountain Andean catchment from satellite optical tristereoscopic remote sensing, Water Resources Research, doi/10.1029/2019WR024880, 2019.

Shaw, T., Caro, A., Mendoza, P., Ayala, Á., Gascoin, S., and McPhee, J.: The Utility of Optical Satellite Winter Snow Depths for Initializing a Glacio-Hydrological Model of a High-Elevation, Andean Catchment, Water Resources Research, doi.org/10.1029/2020WR027188, 2020.

Shean, D.: High Mountain Asia 8-meter DEM Mosaics Derived from Optical Imagery, Version 1. Boulder, Colorado USA. NASA National Snow and Ice Data Center Distributed Active Archive Center, doi: doi.org/10.5067/KXOVQ9L172S2, 2017.

https://doi.org/10.5194/tc-2022-191
Preprint. Discussion started: 4 October 2022

Shean, D. E., Alexandrov, O., Moratto, Z. M., Smith, B. E., Joughin, I. R., Porter, C., and Morin, P.: An automated, open-source pipeline for mass production of digital elevation models (DEMs) from very-high-resolution commercial stereo satellite imagery, ISPRS Journal of Photogrammetry and Remote Sensing, 116:101–117, doi.org/10.1016/j.isprsjprs.2016.03.012, 2016.

Smith, B., Fricker, H. A., Holschuh, N., Gardner, A. S., Adusumilli, S., Brunt, K. M., Csatho, B., Harbeck, K., Huth, A., Neumann, T., Nilsson, J., and Siegfried, M. R.: Land ice height-retrieval algorithm for NASA's ICESat-2 photon-counting laser altimeter, Remote Sensing of Environment, 233, doi.org/10.1016/j.rse.2019.111352, 2019.

Sturm, M., Goldstein, M. A., and Parr, C.: Water and life from snow: A trillion dollar science question, Water Resources Research, 41(1):3534–3544, doi.org/10.1002/2017WR020840, 2017.

Treichler, D. and Kääb, A.: Snow depth from ICESat laser altimetry — A test study in southern Norway, Remote Sensing of Environment, 191:389–401, doi.org/10.1016/j.rse.2017.01.022, 2017.